

Study of Heat Conductivity in DED of TEXTOR-94 Using Multiple Coordinate System Approach.

A. Runov¹, D. Reiter¹, S. Kasilov²

M. F. Heyn, W. Kernbichler³, A.Kaleck⁴

¹ Institut für Laser und Plasmaphysik, Heinrich Heine Universität Düsseldorf

² Institute of Plasma Physics, Kharkov, Ukraine

³ Technische Universität Graz, Austria

⁴ Institut für Plasmaphysik, Forschungszentrum Jülich GmbH

EURATOM Association, Trilateral Euregio Cluster

1. Introduction.

Particle and energy transport in perturbed magnetic fields have been investigated theoretically for a long time (see, e.g., review paper [1]). If one uses an *ad hoc* ansatz for the anomalous transport normal to the field lines (e.g., Bohm-like diffusivities), transport phenomena can readily be studied, by computational means, in two limiting cases: first, in regions of intact magnetic surfaces one can use a “global” magnetic coordinate system aligned to the magnetic surfaces. Secondly, in regions of fully developed ergodicity of the magnetic field one can use stochastic arguments, e.g., the concept of magnetic field diffusivity [2]. In the present paper the 3D Monte Carlo fluid code E3D [3], is employed to address this transport problem in the important intermediate range of partially intact, partially destroyed flux surfaces and a mixture of islands and ergodic zones. We study here heat transport in the boundary plasma layer of the TEXTOR tokamak, with magnetic perturbations produced by the Dynamic Ergodic Divertor [4].

As a special feature of our microscopic modelling of a 3D plasma fluid equation we are able, distinct from any other computational approach, to separate contributions to heat fluxes by their physical origin. In particular we compare the relative importance of field line diversion and field line ergodisation on the enhanced radial transport, in the presence of solid boundaries (open field lines). We show that the field line diversion effect will be dominant in TEXTOR under DED operation.

2. Transport model.

The model is based upon the Braginskii heat balance equation,

$$\frac{\partial u_\alpha}{\partial t} + \nabla \cdot \left[(\mathbf{V}_{\perp\alpha} + \mathbf{h}V_{\parallel\alpha}) u_\alpha - D_{\perp\alpha} \nabla u_\alpha - (D_{\parallel\alpha} - D_{\perp\alpha}) \mathbf{h} \mathbf{h} \cdot \nabla u_\alpha \right] = -\nu_\alpha u_\alpha + S_\alpha^{(u)}.$$

Here index $\alpha = e, i$ stands for the sort of particles (electrons and ions), $u_\alpha \equiv 3nT_\alpha/2$ and T_α are the internal energy and temperature of the species α respectively, n is

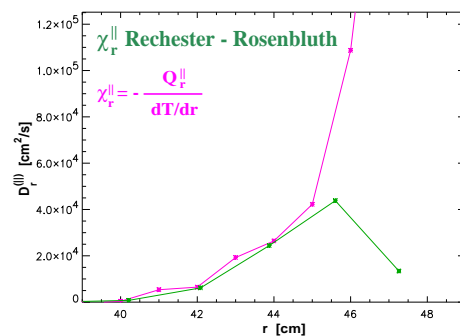


Figure 1: Effective $D_r^{(||)}$, $\varepsilon = 0.1$, $T_{eb} = 50eV$

the plasma density, $\mathbf{h} = \mathbf{B}/B$ is a unit vector along the magnetic field and $\mathbf{V}_{\perp\alpha} \equiv \left(1 - \frac{D_{\perp\alpha}}{D_{\perp}}\right) \mathbf{V}_{\perp}$, $V_{\parallel\alpha} \equiv V_{\parallel} + \frac{1}{n} D_{\parallel\alpha} \mathbf{h} \cdot \nabla n$, $D_{\perp\alpha} \equiv \frac{2\kappa_{\perp\alpha}}{3n}$, $D_{\parallel\alpha} \equiv \frac{2\kappa_{\parallel\alpha}}{3n}$, are the perpendicular and parallel velocities and diffusion coefficients of the internal energy of respective particles, $\kappa_{\perp\alpha}$ and $\kappa_{\parallel\alpha}$ are the anomalous perpendicular and the classical parallel thermal conductivity coefficients, V_{\parallel} is the parallel fluid velocity and \mathbf{V}_{\perp} is the perpendicular fluid velocity due to anomalous particle diffusion connected with D_{\perp} . In order to separate the purely geometrical effects, we restrict ourselves to electron heat conduction only, and treat here the case with constant plasma density, $n_e \equiv 10^{13} \text{ cm}^{-3}$, zero plasma fluid velocity, $\mathbf{V} = 0$, zero heat source/sink rates $S_e^{(u)} = \nu_e = 0$ and constant ‘‘intrinsic’’ anomalous diffusion coefficient $D_{\perp} \equiv 3 \text{ m}^2/\text{s}$. For the same reason, we assume that $\kappa_{\parallel e}$ is constant corresponding to the given ‘‘background’’ plasma temperature $T_e = T_{eb}$ (has been varied $25 \div 75 \text{ eV}$). The computational region in these examples corresponds to the edge plasma region of TEXTOR between the ‘‘core’’ plasma region with boundary at minor radius $r = 38.5 \text{ cm}$ and the wall located at $r = 49 \text{ cm}$. An electron heat flux of 250 kW is assumed at the first boundary and $T_e = 0$ is assumed at the wall.

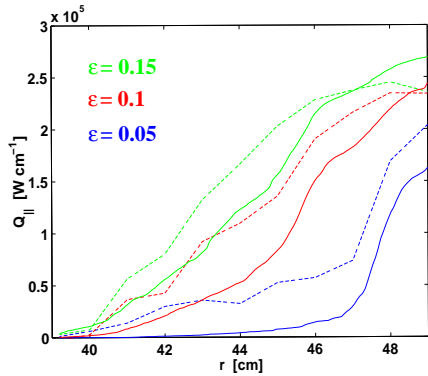


Figure 2: $Q_r^{(\parallel)}$ vs. amplitude of perturbation. Dashed line - E3D, solid line - laminar model.

We solve this equation by means of Multiple Coordinate System Approach (MCSA) [3]. The main idea of the MCSA lies in the partition of the computational domain into a set of sub-domains, each with a typical field line length less than the Kolmogorov length. In each of these sub-domains a separate local magnetic coordinate system is introduced and the connection between two neighboring local coordinate systems is accomplished by means of the ‘‘interpolated cell mapping’’ technique [5]. In contrast to our recent work [3] where the parallel motion is described by a discrete random process, here a continuous random walk process is used. Numerically, this provides a better flexibility for the code.

3. Modeling with E3D.

In this work we use both a simple analytical model of the magnetic field [6] and also magnetic fields computed numerically by the DIVA-GOURDON combined code [4]. The simple model describes most of the main features of the real configuration including unperturbed magnetic surfaces, chains of islands and regions with strong ergodicity by varying of the amplitude of perturbation $\varepsilon = 0.05 \div 0.15$. It still allows comparison with the results of an analytical theory of two possible mechanisms of perturbation-induced transport. The first mechanism is due to the ‘‘diversion’’ of field lines which, in particular, takes place in the scrape-off layer of the usual tokamak divertor and leads to an extension of the radial region containing field lines with connection to the wall. This provides an

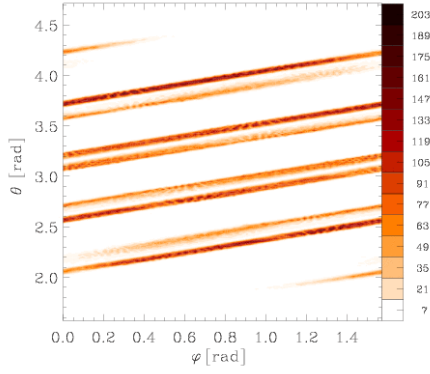


Figure 3: *Steady-state heat load pattern on the wall, model field.*

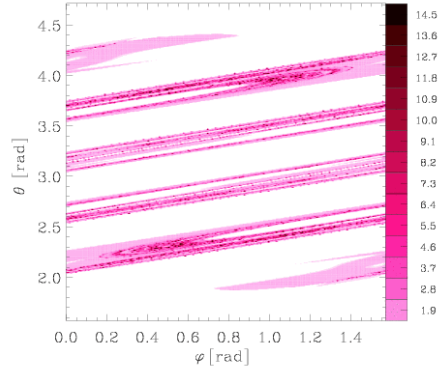


Figure 4: *lg(L_c/L_k) for field lines started from the wall.*

effective heat sink due to the fast parallel transport along those field lines. The second mechanism is due to the “braiding” of field lines that causes an increase of transport due to the combined effect of the fast parallel transport and slow perpendicular transport which de-correlates the electron positions from the field lines [2]. In order to identify the additional transport in more physical terms, two simplified models corresponding to two opposite limiting cases of transport are considered. The Rechester-Rosenbluth diffusion model [2] describes the amplification of the radial heat conductivity because of “braiding” effect, $D_r^{(RR)} = D_{st} D_{\parallel e} \left[L_K \ln \left(\frac{1}{rk_\theta} \left(\frac{D_{\parallel e}}{D_\perp} \right)^{1/2} \right) \right]^{-1}$, where D_{st} is the field line diffusion coefficient and $k_\theta = m/r$ is the characteristic perpendicular wavenumber and L_K is the Kolmogorov length. The “laminar” sink model describes the pure “diversion” effect. Provided we have a self-consistent temperature profile (e.g., calculated with E3D) on the toroidal cut $\varphi = 0$, the flux through $r = const$ can be expressed as an integral from the flux density through the cut:

$$Q_{\parallel}(r) = 2\kappa_{\parallel e} \int_{r_c}^{r_w} dr' r' \int_{-\pi}^{\pi} d\theta \frac{T_e(r', \theta) \Theta(r_{mid}(r', \theta) - r)}{L_c(r', \theta) N_t(r', \theta; r)}.$$

Here, r_c is the core plasma radius, $r_{mid}(r', \theta)$ is the midpoint radius of the field line passing through $\varphi = 0$ at the point (r', θ) , $\Theta(x)$ is the Heaviside step function, $N_t(r', \theta; r)$ accounts for the fact, that a single field line, if followed long enough, can cross the selected toroidal cut more than once, i.e., it is the number of field line crossings through the toroidal cut. L_c is the connection length (distance between the point on the section $\varphi = 0$ and the wall along field line).

The comparison of the E3D computations of Q_{\parallel} with the results of these two models shows that the “laminar” mechanism dominates in TEXTOR DED. Indeed, the Rechester-Rosenbluth coefficient describes the heat transfer satisfactory far from the wall (Fig.1), but the overall parallel heat flux in radial direction shows the good agreement with the laminar model (Fig.2).

The origin of the main heat load at the wall is illustrated in Fig.4, where the logarithm of “area stretching factor” $\sqrt{\mu}$ is plotted as a function of initial field line position on the wall. For the field lines with large connection length L_c , this coefficient is $\sqrt{\mu} \approx \exp(L_c/L_K)$ with L_K the Kolmogorov length. Comparing Figs.3 and 4, one can see that the position of regions with the main heat load correlates with the position of regions where $\sqrt{\mu} > 30$, i.e., it is occupied by field lines steaming from the ergodic zone. This result is a consequence of the consistent treatment of transport in both the ergodic and the laminar zone, without any artificial separation of regions. It is distinctly different from the results of a strongly simplified treatment of the laminar zone alone [7]. This shows the intrinsic complexity of the problem, which appears not to be reducible by simple considerations. To reduce the strong peaking of the power load onto the target (see

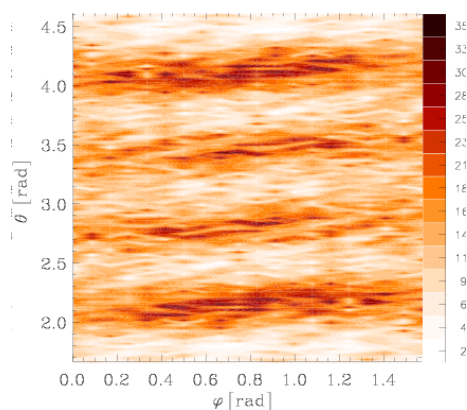


Figure 5: *Time-averaged heat load pattern on the wall, real field.*

Fig.3), the dynamic mode is planned [4]. To estimate the efficiency of smearing out the pattern, the more realistic magnetic configuration provided by the DIVA-GOURDON code is used. In the low frequency limit (if the temperature relaxation is faster than the change of the field, $\omega(r_{max} - r_{min})^2/D_{\perp} \ll 1$) we can employ E3D separately for each phase of supply voltage in turn and then obtain the time averaged profile of the heat transfer onto the bumper limiter (see Fig.5). The time-averaged peak heat flux density on the bumper limiter is reduced by one order of magnitude. However, the heat flux density itself remains poloidally modulated.

Acknowledgements.

This work has been partly carried out within the Association EURATOM-ÖAW and with support from the Österreichisches Bundesministerium für Bildung, Wissenschaft und Kultur under contract number GZ 4229/1-III/5/99.

References.

1. Ph. Ghendrih *et al.*, Plasma Phys. Control. Fusion, **38** 1653 (1996)
2. A. B. Rechester and M. N. Rosenbluth, Phys. Rev. Lett, **40**, 38(1978)
3. A. M. Runov, D. Reiter, and S. V. Kasilov, in *25th EPS Conference on Controlled Fusion and Plasma Physics, 29 June - 3 July, 1998, Prague, Czech Republic, ECA* (European Physical Society, Petit-Lancy, 1998), Vol. 22C, p. 1812.
4. K. H. Finken *et al.*, Fusion Engineering and Design, **37**, 1 (1997)
5. B. H. Tongue, Physica D **8**, 401 (1987).
6. S. S. Abdullaev et al, Phys. Plasmas, **5** 196 (1998)
7. K.H. Finken, T.Eich, and A.Kaleck, Nucl. Fusion **38**, 515 (1998).